Supporting Information

Khan et al. 10.1073/pnas.1212513110

SI Experimental Procedures

Fly Stocks. Following fly stocks were used: lgl^4 (1), $scrib^2$ (2), $scrib^{vartul}$ (3); the latter two represent genetic null alleles of *scrib*; ft^{fd} (4), *UAS-tkv*^{QD} (5), *UAS-yki* (6), *UAS-dsh* (7), *UAS-EGFR*$^{\lambda top}$ (8), *UAS-ras*^{V12} (9), *UAS-hth-GFP* (10), *vkg-GFP* (11), *UAS-vg* (12). *Df(3L)H99* (13), *Minute arm-lacZ FRT40* [Bloomington *Drosophila* Stock Centre (BDSC)], *hs-flp tub-Gal4 UAS-GFP; tub-Gal80 FRT40A* (BDSC) and *FRT82B Minute Ubi-GFP* and *UAS-hth-RNAi* (34637, BDSC).

Methods of Clone Generation. Somatic clones were generated by *flp*/*FRT*, *MARCM*, or *flip-out* techniques. Strategy for clone generation in *Minute* (*M*) background is provided in Fig. S1*C*. Briefly, fly stocks were raised at 25 ± 1 °C or 29 ± 1 °C. Loss-of-function and gain-of-function clones were generated by *flp*/*FRT* (14) and *flip-out* (15) techniques, respectively. *MARCM* technique (16) was used for simultaneous gain-of-function of one gene with loss-of-function of another gene. Staged embryos were collected for 6 h; heat shock was given at 37 °C for 30 min to induce *hs-flp*–mediated somatic recombination. To induce smaller clones for their proximal-distal spatial resolution, heat shock was given for 4 min (for *MARCM* clones) and 10 min (for lgl^- M^+ clones generated in M^+/M^-; *H99*/+ context). Clones were induced as per the scheme presented in Fig. S1*C*.

Genotypes of Clones. The core genotypes relevant to the study are marked in boldface

Clones generated in wild-type background:

***lgl*$^-$** *: w hs-flp; lgl*^{4} *FRT40/Ubi-GFP FRT40*

Clones generated in genetic backgrounds that alleviate tissue surveillance/cell competition (M^+M^-), cell death (*H99*), or both (*H99*; M^+M^-):

lgl*$^-$ *M*$^+$ *in M*$^-$*/M*$^+$: y w hs-flp; lgl*^{4} *FRT40/M arm-lacZ FRT40*

y w hs-flp; lgl^4 *vkg-GFP FRT40/M arm-lacZ FRT40*

y w hs-flp; lgl^4 *FRT40/M ubi-GFP FRT40; diap1-lacZ/+*

scrib*$^-$ *M*$^+$ *in M*$^-$*/M*$^+$: y w hs-flp; scrib*^{2} *FRT82B/M arm-lacZ FRT82B***

y w hs-flp; scrib^2 *FRT82B/M ubi-GFP FRT82B*

lgl*$^-$ *in H99/+:* *y w hs-flp tub-Gal4 UAS-GFP; lgl*^{4} *FRT40/tub-Gal80 FRT40; Df(H99) FRT82/ +

lgl*$^-$ *M*$^+$ *in M*$^+$*/M; H99/ +:* *y w hs-flp; lgl*^{4} *FRT40/M arm-lacZ FRT40 ; Df(H99) FRT82/+

Clones with overexpression of signaling pathway members or transcription factor:

lgl*$^-$ *UAS-yki *: y w hs-flp tub-Gal4 UAS-GFP; lgl*^{4} *FRT40 UAS-yki/tub-Gal80 FRT40*

lgl*$^-$ *UAS-dsh *: y w hs-flp tub-Gal4 UAS-GFP; lgl*^{4}*FRT40/tub-Gal80 FRT40; UAS-dsh*

***lgl*$^-$ *UAS-tkv*^{QD}** *: y w hs-flp tub-Gal4 UAS-GFP; lgl*^{4}*FRT40/ tub-Gal80 FRT40; UAS-tkv*^{QD}

***lgl*$^-$ *UAS-EGFR*$^{\lambda top}$** *: y w hs-flp tub-Gal4 UAS-GFP; lgl*^{4} *FRT40/tub-Gal80 FRT40; UAS-EGFR*$^{\lambda top}$

lgl*$^-$ *ft *: y w hs-flp: lgl*^{4} *ft*^{fd} *FRT40/Ubi-GFP FRT40*

lgl*$^-$ *UAS-ras*^{V12}: y w hs-flp tub-Gal4 UAS-GFP; lgl*^{4}*FRT40 UAS-Ras*^{v12}*/tub-Gal80 FRT40*

lgl*$^-$ *UAS-hth *: y w hs-flp tub-Gal4 UAS-GFP; lgl*^{4}*FRT40/tub-Gal80 FRT40; UAS-hth-GFP/+*

lgl*$^-$ *UAS-vg: *y w hs-flp tub-Gal4 UAS-GFP; lgl*^{4}*FRT40/tub-Gal80 FRT40; UAS-vg/+*

lgl*$^-$ *UAS-yki; UAS-vg: *y w hs-flp tub-Gal4 UAS-GFP; lgl*^{4}*FRT40 UAS-yki/tub-Gal80 FRT40; UAS-vg/+*

Down-regulation of *hth* in lgl^- and $scrib^-$ clones:

lgl*$^-$ *UAS-hth-RNAi *: y w hs-flp tub-Gal4 UAS-GFP; lgl*^{4}*FRT40/ tub-Gal80 FRT40 ; UAS-hth-RNAi*

***scrib*$^-$** *UAS-hth-RNAi: y w hs-flp tub-Gal4 UAS-GFP/+;+; scrib*^{2} *UAS-hth-RNAi/tub-Gal80 FRT82B*

Control clones:

UAS-yki: *w hs-flp: UAS-yki/act>y*$^+$*>Gal4 UAS-GFP*

UAS-dsh: *w hs-flp: act>y*$^+$*>Gal4 UAS-GFP/+; UAS-dsh/+*

***UAS-EGFR*$^{\lambda top}$:** *w hs-flp: act>y*$^+$*>Gal4 UAS-GFP/+; UAS-EGFR*$^{\lambda top}$ */+*

***UAS-Tkv*^{QD}:** *w hs-flp: act>y*$^+$*>Gal4 UAS-GFP/+; UAS-Tkv*^{QD}*/+*

UAS-vg: *w hs-flp: act>y*$^+$*>Gal4 UAS-GFP/+; UAS-vg/ +*

Clone Area Analysis. Desired area was measured using ImageJ software; single optical sections that displayed maximum clonal territory per disc were used for analysis. Percent clone area in a domain (proximal or distal) was calculated as: Total clone area/domain area × 100; percent transformed area in a domain was calculated as: Transformed area/domain area × 100. Mean values of eight discs for each sample were used to plot the graphs (Fig. 1*F*).

Immunofluorescence and Microscopy. Primary antibodies: rabbit anti-caspase-3 (1:500, Sigma-Aldrich), Guinea pig anti-Dlg (1:500; Peter Bryant, University of California, Irvine), Rabbit anti-Distalless (Dll) (1:100; Sean Carroll, University of Wisconsin-Madison, WI), Mouse anti-Elav (1:20; DSHB), Rabbit anti-Ex (1: 1000; Allen Laughon, University of Wisconsin-Madison), Rabbit anti-Homothorax (Hth) (1:500; Henry Sun, Institute of Molecular Biology, Taipei, Taiwan), Goat anti-Hth (1:50; Santa Cruz Biotechnology), Mouse anti-Matrix metalloproteinase-1 (MMP1) (mixed 1:1:1; diluted to 1:100; DSHB-3B8, 5H7 and 23G1), Rabbit anti-Vestigial (Vg) (1:50; Sean Carroll), Mouse anti-Wingless (Wg) (1:1000; DSHB), rabbit anti–β-Gal (1:4,000; ICN Biochemical), Mouse anti–β-gal (1:4,000; Boehringer-Mannheim), Mouse anti-Nubbin (1:50, Steve Cohen, Institute of Molecular and Cell Biology, Singapore), Rat anti-Spalt (1:50; Jose F. de Celis, Autonomous University of Madrid, Spain), and Rat anti-Cut (1:50; DSHB). Secondary antibodies: AlexaFluor 488, 555, and 633. Phalloidin-AlexaFluor 633 for F-actin staining and TOPRO for nuclear marking were used (Invitrogen). Images were acquired with Leica-SP5 Confocal microscope and processed using Leica Confocal Software-LAS AF and Adobe Photoshop.

Microarray, Gene-Set Enrichment Analysis, and Quantitative RT-PCR. ***Microarray.*** Whole-genome transcriptional profiling was done on an Affymetrix platform. In brief, wing discs carrying *lethal giant larvae* (lgl^-) (day 7.5, test) or wild-type (day 4, control) clones, generated in M^+M^- background were used for RNA isolation.

Choice of this time point (day 7.5) for the test sample was guided by the fact that at this stage mosaic discs were largely comprised of proximally transformed $lgl^{-}M^{+}$ clones, whereas distally these were largely extruded (Fig. 1). Total RNA was isolated in triplicates for each genotype using Qiagen RNeasy columns. Next, 1.5 μg of RNA from each of the test and control samples were converted to cRNA and hybridized to Affymetrix *Drosophila* Genome 2.0 array, according to the manufacturer's instructions, and scanned with Affymetrix GeneChip Scanner 3000. Feature extraction and quality control was performed on Affymetrix gene chip operating software. The correlation coefficients for the replicates were >0.95, which gave a measure of their agreement. The 3′/5′ ratio for the control genes, GAPDH and Actin was <2.5, which ascertained the integrity of the RNA used for hybridization. Following the widely accepted assumption that there are no significant differences in the overall intensities of the test and baseline arrays, we scaled the target intensities of each array to the TGT value 500. In each of the six cases (three each for test and baseline arrays), the scaling factor was below 3, which met manufacturer's recommendations for making the assumption mentioned above. Raw CEL files of arrays were normalized by Robust Multiarray Average method using GenePattern software, following background correction (http://www.broadinstitute.org/cancer/software/genepattern). CEL files and processed .gct files (output files from GenePattern) have been submitted to ArrayExpress (http://www.ebi.ac.uk/arrayexpress/experiments/E-MEXP-2753/).

Gene-set enrichment analysis. Gene-set enrichment analysis (GSEA) provides a quantitative measure for the status of a predefined set of genes between two phenotypes being compared. It calculates an normalized enrichment score (NES) using running sum statistics, which could be positive or negative depending on the correlation of the genes in the gene-set with the phenotype under study. The processed .gct file from GenePattern served as an input for the GSEA. Gene sets for signaling pathways were obtained from Gene Ontology (GO), and included: Wg/Wnt receptor signaling pathway (GO: 0016055), Epidermal Growth Factor Receptor Signaling Pathway (GO: 0007173), and Transforming Growth Factor-β Signaling Pathway (GO: 0007179). Members of the Hippo pathway were curated from recent publications. Those genes for which corresponding probes were not found in the *Drosophila* Genome 2.0 array were excluded from their respective gene-sets. Because the source of our sample was *lgl* mutant discs, we excluded *lgl* from gene-sets of signaling pathways that included it. GSEA analyses were carried out using the following parameters and genes were ranked based on comparison of phenotypes: *lgl* (test) vs. control (wild-type) mosaics, using signal-to-noise metric. The enrichment score was calculated using weighted running sum statistics and we used gene-based permutation ($n = 1{,}000$) to calculate the nominal P value. To correct for multiple-hypothesis testing, we took the false-discovery rate (FDR) value into consideration. GSEA provides P value, a measure of statistical significance for the calculated enrichment score as well as FDR (q-value) and the more conservative family-wise error rate, corrections for multiple hypothesis testing. We considered a pathway enriched only at $P < 0.05$. Hippo (NES = 2.02, $P < 0.001$, q < 0.001), Wg (NES = 1.82, $P < 0.001$, q = 0.003), TGF-β (NES = 1.78, $P = 0.002$, q = 0.003), and EGFR (n = 1.49, $P = 0.040$, q = 0.042) were found enriched.

Quantitative RT-PCR. RT-PCR was performed using SYBR green from Applied Biosystems (ABI) on ABI7 900 HT. In brief, total RNA from test (*lgl* mutant mosaic) and control (lgl^{+} mosaic) wing imaginal discs were isolated using Qiagen RNeasy columns. RNA was treated with RNase free DNase (Roche), to get rid of any traces of DNA, before converting it to cDNA (using cDNA preparation kit from ABI). The resulting cDNA was used as substrate for relative quantitation using SYBR green on ABI7 900 HT. β-Tubulin served as endogenous controls. Genes were assayed from four to six biological replicates for test and control. The specifications of the run were as follows: DNA polymerase activation for 10 min at 95 °C, followed by 40 cycles of duplex melting for 15 s at 95 °C and a combined annealing and extension step for 1 min at 60 °C. The threshold-cycle (Ct) values were automatically generated. The relative expression value of each gene in the test as against the control samples was calculated by $2^{-\Delta\Delta Ct}$ method. Sequences of forward and reverse primers are given below:

dMyc (F: 5′ acacgcgctgcaacgatatgg 3′, R: 5′ cgagggatttgtgggtagcttctt 3′), *kibra* (F: 5′ gcaggcccagcatagcaaactc 3′, R: 5′ caggcggccaccaagggat 3′), *expanded* (F 5′ gccgcctttacctgtccaac 3′, R: 5′ cgttccggtttccaattagct 3′), *wingless* (F: 5′ tgatggccctgtgcagcg 3′, R: 5′ caccacatggagccccgg 3′), *Wnt4* (F: 5′ cagcgatcaatgcgacaggtgt 3′, R: 5′ gtgaccgcgcagtaggaggg 3′), *dally* (F: 5′ ccaccatcgacaagagcaaggag 3′, R: 5′ gctgagtgtagtccccgaaacga 3′), *pangolin* (F: 5′ tgcgcctgatttaaagtacaaaatgtg 3′, R: 5′ tttattcatcaaagcacaattgggtg 3′), *vein* (F: 5′ tgccaaaaacccatcacc 3′, R: 5′ aggcgaggggaattgtacga 3′), *spitz* (F: 5′ tctcgtccatgtccggcac 3′, R: 5′ attgggcctgggcgtggtc 3′), *dawdle* (F: 5′ cggtgctaacaagtcgctggagt 3′, R: 5′ tgggcagcgtcttcaccgtc 3′), *short gastrulation* (F: 5′ tgatgtcccacggcgagcag 3′, R: 5′ acgccgcttgctggtcacg 3′), *thickveins* (F: 5′ tgcatgcctcccgaagacaac 3′, R: 5′ ggggtacaggtcacggttgca 3′), *β Tubulin 56D* (F: 5′ caagctggtcagtgcggcaac 3′, R: 5′ gctgtcaccgtggtaggcgcc 3′).

1. Gateff E (1978) Malignant neoplasms of genetic origin in *Drosophila* melanogaster. *Science* 200(4349):1448–1459.
2. Bilder D, Perrimon N (2000) Localization of apical epithelial determinants by the basolateral PDZ protein Scribble. *Nature* 403(6770):676–680.
3. Li M, Marhold J, Gatos A, Torok I, Mechler BM (2001) Differential expression of two *scribble* isoforms during *Drosophila* embryogenesis. *Mech Dev* 108(1-2):185–190.
4. Bryant PJ, Huettner B, Held LI, Jr., Ryerse J, Szidonya J (1988) Mutations at the fat locus interfere with cell proliferation control and epithelial morphogenesis in *Drosophila*. *Dev Biol* 129(2):541–554.
5. Nellen D, Burke R, Struhl G, Basler K (1996) Direct and long-range action of a DPP morphogen gradient. *Cell* 85(3):357–368.
6. Huang J, Wu S, Barrera J, Matthews K, Pan D (2005) The Hippo signaling pathway coordinately regulates cell proliferation and apoptosis by inactivating Yorkie, the *Drosophila* Homolog of YAP. *Cell* 122(3):421–434.
7. Neumann CJ, Cohen SM (1997) Long-range action of Wingless organizes the dorsal-ventral axis of the *Drosophila* wing. *Development* 124(4):871–880.
8. Queenan AM, Ghabrial A, Schüpbach T (1997) Ectopic activation of torpedo/Egfr, a *Drosophila* receptor tyrosine kinase, dorsalizes both the eggshell and the embryo. *Development* 124(19):3871–3880.
9. Karim FD, Rubin GM (1998) Ectopic expression of activated Ras1 induces hyperplastic growth and increased cell death in *Drosophila* imaginal tissues. *Development* 125(1):1–9.
10. Casares F, Mann RS (2000) A dual role for homothorax in inhibiting wing blade development and specifying proximal wing identities in *Drosophila*. *Development* 127(7):1499–1508.
11. Morin X, Daneman R, Zavortink M, Chia W (2001) A protein trap strategy to detect GFP-tagged proteins expressed from their endogenous loci in *Drosophila*. *Proc Natl Acad Sci USA* 98(26):15050–15055.
12. Kim J, et al. (1996) Integration of positional signals and regulation of wing formation and identity by *Drosophila* vestigial gene. *Nature* 382(6587):133–138.
13. White K, et al. (1994) Genetic control of programmed cell death in *Drosophila*. *Science* 264(5159):677–683.
14. Xu T, Rubin GM (1993) Analysis of genetic mosaics in developing and adult *Drosophila* tissues. *Development* 117(4):1223–1237.
15. Struhl G, Basler K (1993) Organizing activity of wingless protein in *Drosophila*. *Cell* 72(4):527–540.
16. Lee T, Luo L (1999) Mosaic analysis with a repressible cell marker for studies of gene function in neuronal morphogenesis. *Neuron* 22(3):451–461.

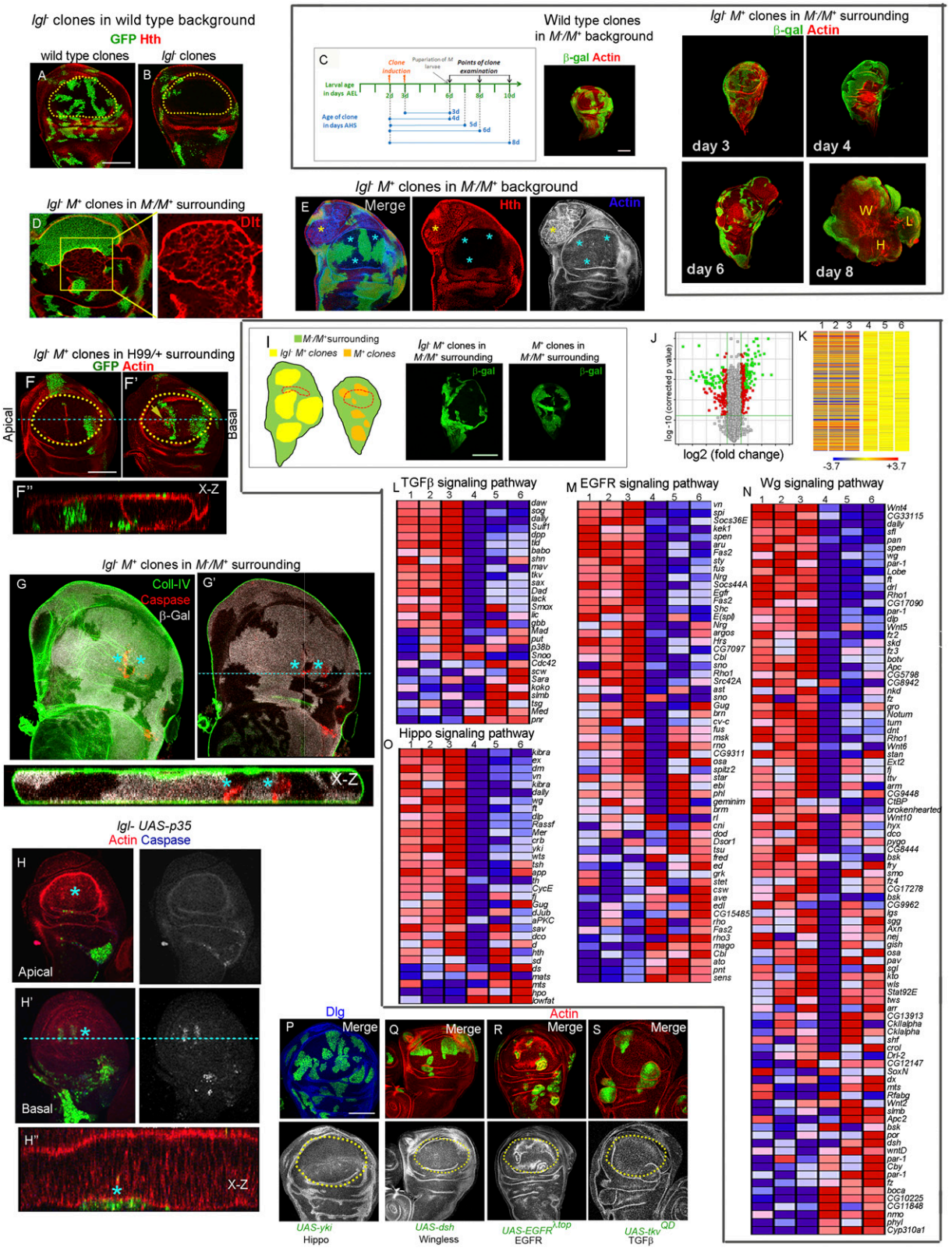

Fig. S1. Neoplasia in *lgl*$^{-}$ clones in wing primordium and their genome-wide transcription profile. (*A* and *B*) Mosaic wing imaginal disc carrying somatic clones, marked by GFP (green): (*A*) wild-type and (*B*) *lgl*$^{-}$ 3-d-old clones; surrounding cells (non-GFP) are all wild-type. Hth (red) expression marks the entire proximal domain of the wing primordium, and its absence marks the distal domain (yellow dotted line). Note the overall low abundance and small size of *lgl*$^{-}$ clones (*B*) compared with their wild-type (*A*) counterparts. (*C*) Strategy for generation and example of *lgl*$^{-}$*M*$^{+}$ clones (absence of GFP) induced in *M*$^{-}$/*M*$^{+}$ surrounding (GFP, green). Mosaic discs were stained with Phalloidin (red) to mark the F-actin cytoskeleton. Clones were induced by heat shock (37 °C, 30 min) of larvae 2 d after egg laying (d AEL). Examination of these clones after 6, 7, 8, and 10 d AEL gave a clonal age of 4, 5, 6, and 8 d, respectively. To obtain clones of a younger age (3 d old), clones were induced 3 d AEL and observed after 6 d AEL. The wild-type mosaic wing imaginal discs were dissected 5 d AEL, shortly before

Legend continued on following page

their pupariation; larvae with the mosaic discs carrying $lgl^{-}M^{+}$ clones fail to pupariate because of tumor load and die as giant larvae. Note that progressive increase in $lgl^{-}M^{+}$ clonal territories with increasing larval age and after 8 d of clone induction, mosaic wing (W), leg (L), and haltere (H) imaginal discs coalesce with each other revealing their invasive transformation. Larval age at the time of heat shock and dissection varied up to ± 3 h. (*D*) lgl^{-} M^{+} clones (unmarked, absence of β-gal) generated in an M^{-}/M^{+} surrounding (β-gal, green) and stained with an apical membrane cell marker, Discs Lost (Dlt, red) (1). Boxed area is shown at a higher magnification in the right to reveal mislocalization of Dlt, and thereby loss of apico-basal polarity in transformed $lgl^{-}M^{+}$ clones. (*E*) $lgl^{-}M^{+}$ clones (unmarked, absence of β-gal) generated in an M^{-}/M^{+} surrounding (β-gal, green) and stained with phalloidin (blue) to mark the actin cytoskeleton, and Hth (red) to mark the proximal domain of the mosaic wing primordium. Mosaic discs were dissected 5 d after heat shock. Note the disruption of actin cytoskeleton (yellow stars) in clones located in the Hth-expressing, proximal (hinge) domain. In contrast, distal $lgl^{-}M^{+}$ clones (blue star) are not transformed, as revealed by their intact cytoarchitecture (F-actin). (*F*–*F*′′) lgl^{-} clones (GFP, green) generated in *H99*/+ (unmarked) background. In the apical plane (*F*) distal lgl^{-} clones are sparsely seen; basally (*F*′) these are seen abundantly (yellow arrow). The *x*–*z* section (*F*′′) of the mosaic disc along the blue dotted line marked in *F* reveals basal extrusion of the lgl^{-} clones. Yellow dotted line marks the distal domain of the wing primordium. Apical-Basal (A←B) orientation in the *x*–*z* sections is shown. (*G* and *G*′) $lgl^{-}M^{+}$ clones (unmarked, absence of β-gal) generated in an M^{-}/M^{+} surrounding (β-gal, gray) shows expression of caspase (red). Basement membrane is marked by collagen-IV-GFP (Col-IV, green). The *x*–*z* section over the dotted line shows the extrusion of caspase-expressing distal $lgl^{-}M^{+}$ clones (blue star) without breaking the basement membrane. Vkg-GFP at the top represents the basement membrane of peripodial cells. (*H*–*H*′′) Cell death in lgl^{-} clones (GFP, green) induced in a wild-type genetic background is not rescued by expressing the baculovirus antiapoptosis protein, p35 (2). Apical sections of a mosaic disc do not reveal distal lgl^{-} *UAS-p35* clones (*H*), while basal sections (*H*′) reveal their basal extrusion and cell death (caspase, gray). The *x*–*z* section along the dotted line showed in *H*′ to further reveal basal extrusion of these clones (green). (*I*–*K*) Genome-wide transcription profile of lgl^{-} mosaic wing imaginal discs. (*I*) Cartoon representation of test $lgl^{-}M^{+}$ (yellow) and M^{+}, control, wild-type (orange) clones generated in M^{-}/M^{+} surrounding (green). The test and control mosaic discs are thus distinct only with respect to the genotype of the clone induced, the surrounding being identical. Red dotted circles represent the distal domains of such mosaic discs. Actual examples of such mosaic discs carrying test (lgl^{-} M^{+}) and control (M^{+}) clones are shown at the right. (*J*) A volcano plot displaying distribution of genes based on their fold-changes and *P* values. Colored dots, altogether 356, represent genes with a fold-change (up- or down-regulation) of ≥ 2 at *P* values of <0.05 (red) and <0.03 (green); gray dots represents those that did not show a significant fold-change. (*K*) Heat-map representing the status of these 356 misregulated genes in three biological replicates each for lgl^{-} (columns 1, 2, 3) and wild-type (columns 4, 5, 6) mosaic samples reveal tight agreement among the replicates. (*L*–*O*) Heat maps showing the transcriptional status of signaling pathway members: TGF-β (*n* = 28, *L*), EGFR (*n* = 60, *M*), Wg (*n* = 92, *N*), Hippo (*n* = 32, *O*), signaling pathways, where *n* represents the number of genes in a given gene-set. Columns 1–3 and 4–6, respectively, depict the gene expression status in three individual replicates of test and control mosaic discs. (*P*–*S*) Up-regulation of signaling pathways alone in somatic clones does not induce neoplastic transformations. Clones (GFP, green) displaying up-regulation of signaling pathways because of overexpression of *UAS-yki* (*P*), *UAS-dsh* (*Q*), *UAS-EGFR*$^{\lambda top}$ (*R*), and *UAS-tkv*^{QD} (*S*) transgenes in wild-type wing primordium. In each case, clones retain their apico-basal polarity, as assayed by either the lateral cell membrane marker, Disc Large, Dlg (*P*, blue) or actin (*Q*–*S*, red). Also note that in each case clones survive in both the proximal and distal domains (yellow broken line) of the wing primordium. [Scale bars (*A*–*H* and *J*–*S*) 100 μm; (*I*), 200 μm.]

1. Bhat MA, et al. (1999) Discs Lost, a novel multi-PDZ domain protein, establishes and maintains epithelial polarity. *Cell* 96(6):833–845.
2. Hay BA, Wolff T, Rubin GM (1994) Expression of baculovirus P35 prevents cell death in *Drosophila*. *Development* 120(8):2121–2129.

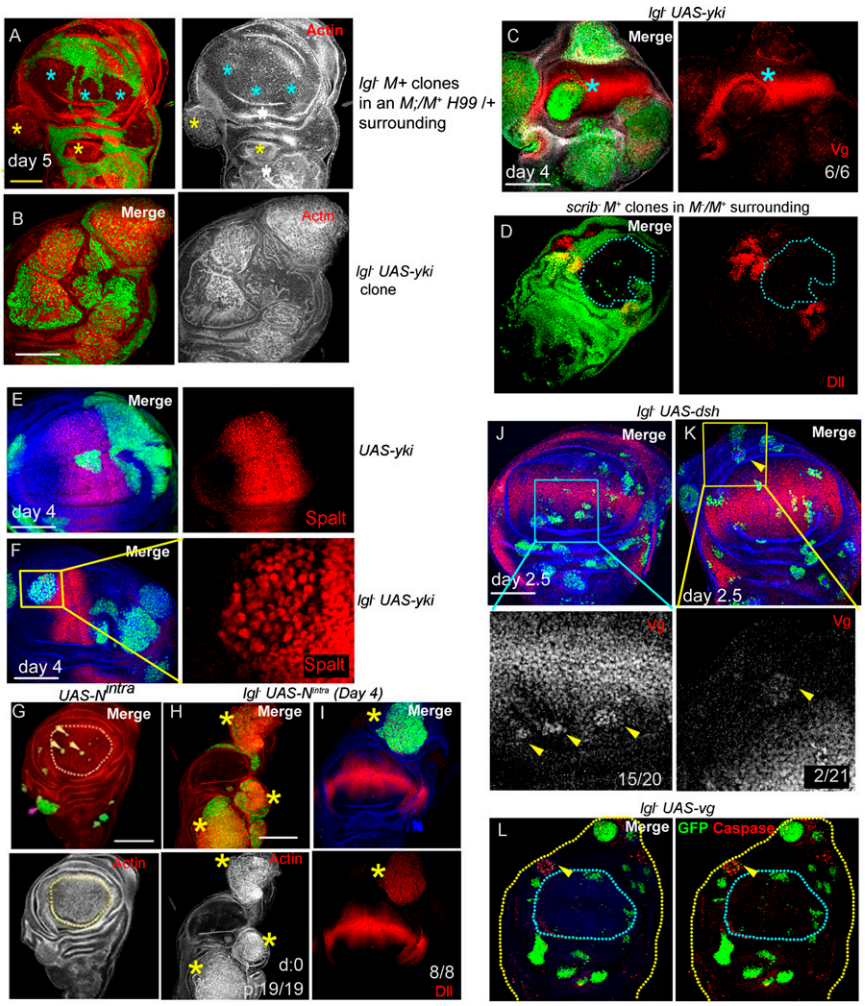

Fig. S2. (*A* and *B*) *lgl*$^{-}$*M*$^{+}$ clones (absence of green, *A*) generated in *M*$^{-}$/*M*$^{+}$*; H99*/+ context display neoplastic transformation in the proximal clones (yellow star) on day 5 (F-actin, red) but distally these were not transformed (blue stars). *lgl*$^{-}$ *UAS-yki* clones (GFP, green, *B*) display massive growth and neoplastic transformation as revealed by their altered actin cytoarchitecture (red). Note the poor demarcation of the proximal and distal origins of these overgrown clones. (*C*) A distal *lgl*$^{-}$ *UAS-yki* clone (green, blue star) displaying complete loss of Vg. (*D*) *scrib*$^{-}$ *M*$^{+}$ clones (absence of GFP, broken line) generated in *M*$^{-}$/*M*$^{+}$ surrounding (day 4) display distal loss of Dll (red). (*E*) Distal gain of Yorkie (Yki) (*UAS-yki*, green) alone or (*F*) in *lgl*$^{-}$ clones (*lgl*$^{-}$ *UAS-yki,* green) does not altered expression of the Dpp signaling target, Spalt (red). Boxed area in *F* is shown at a higher magnification to reveal nuclear expression of Spalt (red) in the clonal area (GFP-positive). (*G–K*) Clones with a gain of N signaling (*UAS-N*^{intra}, green) display poor growth both in distal (within the dotted line, *G*) and in proximal domain, but *lgl*$^{-}$ clones displaying gain of N signaling (*lgl*$^{-}$ *UAS-N*^{intra}, green, *H*) display neoplasia in only the proximal domain (actin, yellow stars) and also activate its target Dll (red, *I*). Distally, however, *lgl*$^{-}$ *UAS-N*^{intra} clones were not recovered (*H* and *I*). (*J–K*) Early stage *lgl*$^{-}$ clones (2.5 d after clone induction) displaying gain of Wg signaling (*lgl*$^{-}$ *UAS-dsh,* green). Note that some of the distal clones (blue box) display gain of Vg (red). Boxed area in *J* is shown at a higher magnification in a panel below, but in the example shown in *K* such a gain of Vg is seen in a clone located in the presumptive hinge (proximal) domain of the wing (yellow box). Boxed area in *K* is shown at a higher magnification in a panel below. (*L*) Cell death in *lgl*$^{-}$*UAS-vg* clones (caspase, red). Few small clones are visible in the distal domain (blue dotted line); clones in the proximal (yellow arrow head) exhibit extensive cell death (caspase, red). All scores pertain to clones in the distal wing unless specified separately as distal (d) and proximal (p). (Scale bars, 100 μm.)

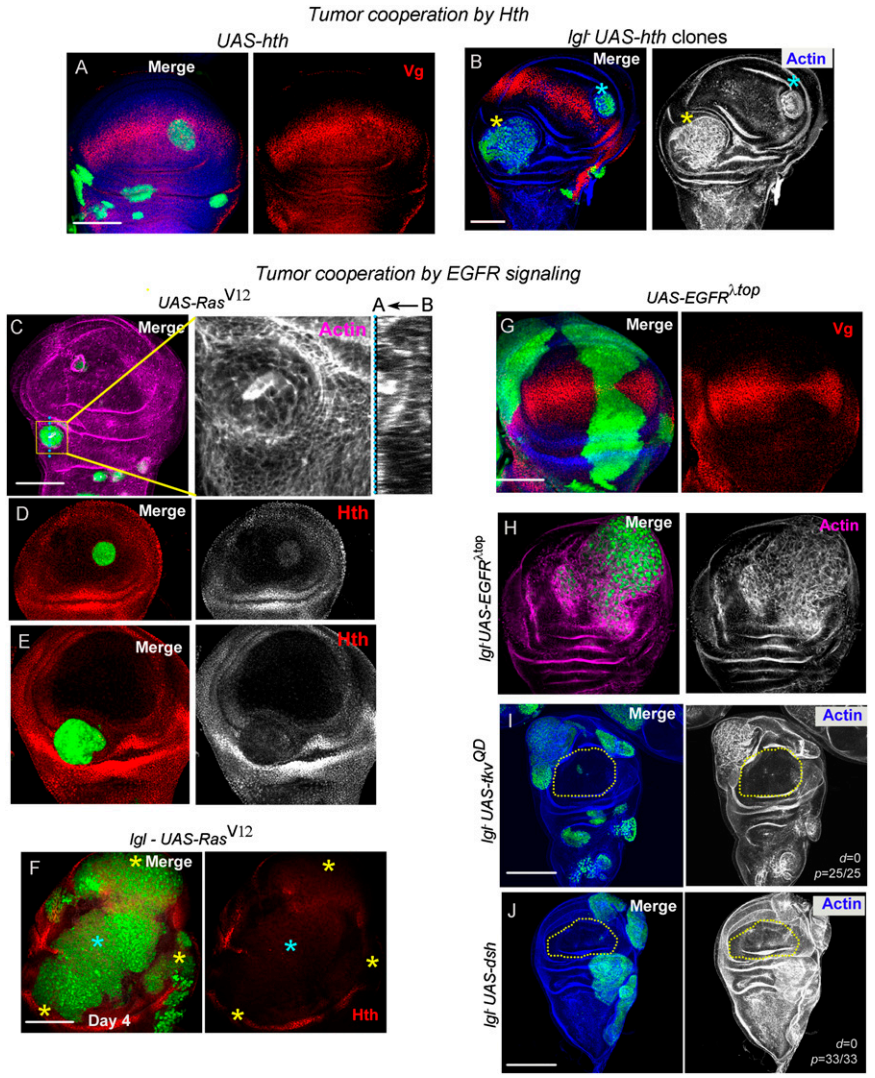

Fig. S3. Hth and Ras/EGFR-mediated *lgl* neoplasia. (*A*) *UAS-hth* clones (GFP, green) display only marginal down-regulation of Vg (Red). (*B*) lgl^{-} *UAS-hth* clones (GFP, green), display only proximal neoplastic transformation (yellow star), and distally these displayed marginal loss of Vg (red) and early signs of actin (blue) disruption (blue star). (*C*) *UAS-ras*^{V12} clones (GFP, green) do not display neoplastic transformation (actin, purple). Cytoarchitecture of the proximal clones (boxed areas) is shown at a higher magnification on the right along with its *x–z* section at the far right. A←B displays apical and basal orientation of the epithelium in X-Z section. (*D*) A *UAS-ras*^{V12} clone displaying distal gain of Hth although proximally (*E*) Hth is down-regulated. (*F*) lgl^{-} *UAS-ras*^{V12} clones (GFP, green) do not display gain of Hth (blue star) in the presumptive distal domain (blue star) but on the hinge domain (yellow stars) these display loss of Hth. (*G*) *UAS EGFR*$^{\lambda top}$ clones display distal loss of Vg. (*H*) Distal transformation (actin, purple) of lgl^{-} *UAS-EGFR*$^{\lambda top}$ clones in cultures raised at 29 °C, while (*I–J*) in those of (*I*) lgl^{-} *UAS-tkv*^{QD} and (*J*) lgl^{-} *UAS-dsh* neoplasia was restricted to only the proximal clones. Yellow dotted line marks the presumptive distal domain; scores of distally (d) and proximally (p) transformed clones are shown. [Scale bars (*A–H*), 100 μm; (*I* and *J*), 200 μm.]